

## Video Sitting Posture Recognition of Human Skeletal Features Based On Deep Learning

Hongmei Yang

School of Information Science and Technology.  
Northeast Normal University  
Changchun, China  
e-mail: yanghm644@nenu.edu.cn

Xiquan Yang

School of Information Science and Technology  
Northeast Normal University  
Changchun, China  
e-mail: yangxq375@nenu.edu.cn

**Abstract** - Sitting in a poor posture for long time can be detrimental to your health. In this regard, video-based detection of poor sitting posture and providing alerts can help people to improve their physical and mental health and productivity. The use of computer vision to detect human sitting posture is a simple method, but there is a problem of low accuracy in practical applications. In this paper, we propose a video sitting detection method based on multidimensional skeletal features of the human body. Using OpenPose to extract human information features from video sequences, global angle information and local angle information formed by human skeletal segments are used as dimensional features, and sitting posture recognition is detected by deep learning with LSTM models. Experiments show that the method effectively improves the accuracy rate.

**Keywords** - deep learning; OpenPose; multidimensional skeletal features; sitting posture recognition

### I. INTRODUCTION

Prolonged poor sitting posture can lead to myopia, hunchback, spinal disorders, lumbar spine disorders [1] and may can influence mental health [2]. This can lead to mental health problems. This is why effective posture detection is so important for improving the quality of life and maintaining physical and mental health. The current applications of sitting posture recognition are mainly to integrate sitting posture recognition into living or learning devices, such as Zheng et al. applied sitting posture recognition to learning machines in order to detect and remind students of their sitting and standing postures [3]. Zhang et al. acquire the image of human sitting posture in real time and output the current user's practice sitting posture, which not only can solve the trouble of no one reminding the user of improper sitting posture when working or studying, but also can simplify the preparation steps for using the sitting posture detection device and effectively remind the user of proper sitting posture so as not to reduce the eyesight [4]. Zhao et al. have used human skeletal points to detect and identify abnormal behavior in a vehicle, providing the possibility of safe driving and early warning [5].

Sitting posture recognition is an important element of human posture recognition. There are two main approaches to human posture recognition at home and abroad: human posture recognition based on mechanical sensors and machine vision. In the 2001, Chandna et al. used principal component analysis to solve the sitting posture classification problem [6]. In 2003 and 2005, Lis et al. differentiation classification algorithms to classify sitting postures using Fisher-Rao discriminant analysis and applied[7]. Zhang et al. used an algorithmic combination approach to recognize different poses of the head[8]. Takafumi et al. used an unsupervised method to identify 16 common human activities with an

accuracy of 80.4%[9]. O'Sullivan et al. designed a real-time feedback system to provide users with goodness of posture by determining the angle of the central axis of the head, left and right shoulder, and horizontal through the information collected by the camera [10]. Aida et al. used a feature fusion algorithm to recognize human hand gestures based on computer vision, which can recognize 37 hand gestures with an accuracy of 98.64%[11]. In 2007, Straker et al. used a sensor placement strategy based on a logistic regression optimization algorithm to place a minimum number of sensors on the human body to obtain information about the human body for sitting [12]. Grandjean, E, H. Z. Tan, M. Zhu, Jaimes, Alejandro, Ribeiro, B, et al. used different types and numbers of sensors to detect and identify sitting postures based on machine learning or deep learning methods to classify a variety of different sitting postures[13]-[19]. For example, Jaimes, Alejandro et al. used 16 force sensors and backrest angles to identify sitting postures based on the features of the Random Forest algorithm with an accuracy of 90%[20].

Although sensor-based methods have achieved high accuracy, these methods suffer from expensive equipment, environmental vulnerability of data acquisition and transmission processes, the need for subject cooperation and poor portability. Therefore, computer vision-based sitting recognition detection is a hot issue for current research.

### II. RELATED WORKS

There are two main approaches for sitting recognition and classification based on machine vision, one is to use HOG, PHOG, LBP and other methods to extract contour features or local texture features of images for sitting recognition and classification. For example, Feng Jing and Jia Ruo Chen used to extract contour features and texture features of images for sitting recognition and classification[21][22]. The other one is

to use human skeletal keypoints data to extract human body information as features for sitting posture recognition and classification. There are two main approaches for acquiring human skeletal keypoints: the Kinect sensor-based and OpenPose based. For example, Shiqi Cai, Li, TL Le et al. extract human skeletal keypoints based on the Kinect sensor and use machine learning or deep learning for sitting posture recognition and classification[23]-[25]. Although the accuracy of human skeletal keypoints extraction using Kinect sensor is high, there are problems such as expensive equipment and susceptibility to environmental impact. The use of OpenPose to extract human skeletal keypoints data will remedy these shortcomings. For example, Chen Kehan used OpenPose to extract human skeletal keypoints and used convolutional neural networks to recognize and classify sitting postures[26]. However, the current use of skeletal data for sitting is not as good as it could be. Most of the sitting posture recognition and classification using skeletal data only uses a single feature, such as using all the data of human keypoints as features, resulting in a low accuracy of sitting posture recognition.

In general, the current sensor-based sitting recognition methods have problems such as expensive equipment, difficulty in data acquisition, susceptibility to environmental factors such as light and temperature, and poor universality; while machine vision-based sitting recognition research methods are relatively few and have the problem of insufficient accuracy caused by using only a single feature.

This paper proposes a method for extracting human keypoints classification features based on OpenPose and using the multi-feature category information formed by human skeletal segments to determine the sitting posture in a continuous time series. Firstly, the data augmentation method is designed to expand the data set, extract the human skeletal keypoints category information in the time series using OpenPose, and determine the sub-features for selecting multiple angles. Secondly, the local angle features formed by the skeletal segments and the global angle features are combined to perform feature fusion and highlight the sitting posture features. Finally, to detect bad sitting posture, the human motion laws optimization algorithm is designed to optimize LSTM Models. Achieved reduced equipment cost and improved accuracy of video-based sitting posture recognition.

Firstly, according to human osteology and rehabilitation medicine, define the standards of correct and poor sitting posture. Then a data augmentation method is designed to expand the dataset in accordance with this paper and use open-source library OpenPose, to extract and save the human keypoints from the continuous sitting images in the video. And fuse the keypoint features, local angle features and global angle features in a serial way. Finally, the LSTM is optimally tuned based on the laws of human sitting to achieve human sitting recognition.

Based on research related to human osteology and efficacy, the correct sitting posture should be to maintain two 90°, feet on the ground, ensuring that the knee joints are presented 90°; the trunk is upright, keeping the thighs and trunk presented 90°[27]. A diagram of healthy sitting posture and poor sitting

posture is shown in the Fig 1. This article focuses on the analysis of poor sitting posture caused by forward leaning, backward leaning, straightening and bending of the legs, etc. and different bending angles of the spine, with forward leaning bending angles of the spine between 10°-90° and backward leaning bending angles between 90°-170°, which is a wide range of representative problems.

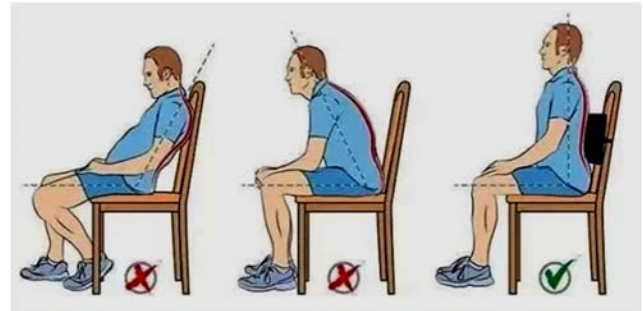


Figure 1. Bad sitting posture vs. healthy sitting posture

### III. SYSTEM DESIGN

#### A. Representation of Skeletal Features

OpenPose can obtain 18 2D coordinate information about the joints of the human body in real time, which can be expressed in  $x, y$ . The skeletal information is represented as  $J = \{j_0, j_1, j_2, \dots, j_N\}$ , where  $j_i = (x_i, y_i)$  represents the coordinate position of key-points,  $0 \leq i \leq 17, N = 17$ . Each skeletal keypoints is shown in the Fig 2.

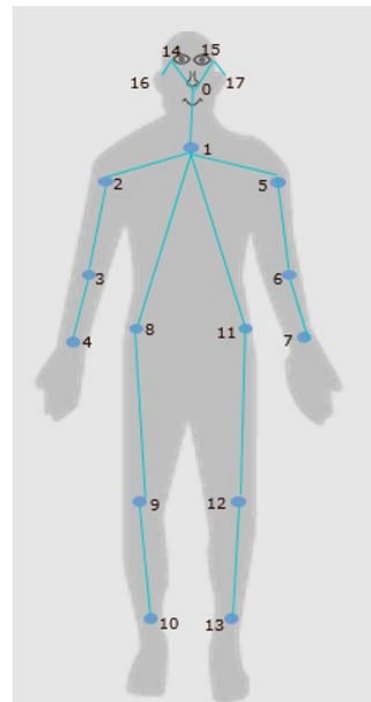


Figure 2. Framework of keypoints of the human skeleton

Any two key points are joined to form a skeletal segment, as shown in the Table 1.

TABEL I. SKELETAL SEGMENTS COMPRISING KEY POINTS OF THE HUMAN BODY

| $S_i$ | Keypoints      | $S_i$    | Keypoints            | $S_i$    | Keypoints            |
|-------|----------------|----------|----------------------|----------|----------------------|
| $S_1$ | $\{j_1, j_2\}$ | $S_7$    | $\{j_1, j_8\}$       | $S_{13}$ | $\{j_1, j_0\}$       |
| $S_2$ | $\{j_1, j_5\}$ | $S_8$    | $\{j_8, j_9\}$       | $S_{14}$ | $\{j_0, j_{14}\}$    |
| $S_3$ | $\{j_2, j_3\}$ | $S_9$    | $\{j_9, j_{10}\}$    | $S_{15}$ | $\{j_{14}, j_{16}\}$ |
| $S_4$ | $\{j_3, j_4\}$ | $S_{10}$ | $\{j_1, j_{11}\}$    | $S_{16}$ | $\{j_0, j_{15}\}$    |
| $S_5$ | $\{j_5, j_6\}$ | $S_{11}$ | $\{j_{11}, j_{12}\}$ | $S_{17}$ | $\{j_{15}, j_{17}\}$ |
| $S_6$ | $\{j_6, j_7\}$ | $S_{12}$ | $\{j_{12}, j_{13}\}$ |          |                      |

Any two key points  $j_a, j_b$  form a skeletal segment between them, define the direction vector of the linear equation for the skeletal segment  $S_i$  as:

$$v_i(v_x, v_y) = (x_b - x_a, y_b - y_a) \quad (1)$$

Two skeletal segments  $S_a, S_b$  angles are defined as:

$$\text{Angle}(S_a, S_b) = \arcsin \frac{v_{xa} * v_{xb} + v_{ya} * v_{yb}}{\sqrt{(v_{xa}^2 + v_{ya}^2) * (v_{xb}^2 + v_{yb}^2)}} \quad (2)$$

Where  $v_a(v_{xa}, v_{ya})$  is the direction vector of  $S_a$ , the  $v_b(v_{xb}, v_{yb})$  is the direction vector of  $S_b$ .

### B. Local and Global Angle Features

In order to solve the problem that a single feature cannot accurately identify sitting posture. We classify human skeletal features into local angle features and global angle features. Among them, the angle information of the representative skeletal segments for judging the sitting posture of the human body are the angle information of the shoulder ankle and ankle plane, the angle information of the body and thigh, and the angle information of the thigh and calf. The first one is the global angle feature and the latter two are local angle features. The angle information formed by the ankle and ankle plane at the shoulder is selected for the experiments in this paper,

$(S_{210}, S_{10 \text{ 平}}), (S_{513}, S_{13 \text{ 平}})$  for the global angle and the angle information of the body thigh  $(S_{1mid}, S_{89}), (S_{1mid}, S_{1112})$  and the angle information of the thigh and calf  $(S_{89}, S_{910}), (S_{1112}, S_{1213})$  for the local angles.  $j_{mid}$  representing midpoint of skeletal keypoints  $j_8$  with the  $j_{11}$ , the  $j_{mid}$  with  $j_1$  form the skeletal segment representing the body:

$$j_{mid} = \left( \frac{x_8 + x_{11}}{2}, \frac{y_8 + y_{11}}{2} \right), j_{\text{平}}$$

represents the plane point, and form the vector of ankles and planes with keypoints  $j_{10}$  and  $j_{12}$ , for  $S_{10 \text{ 平}}, j_{\text{平}} = (j_{10} - 1, 0)$ , for  $S_{13 \text{ 平}}, j_{\text{平}} = (j_{12} + 1, 0)$ .

According to ergonomics and literature [28][29], a healthy sitting posture should have the angle of the body to the

thighs  $Angle_1$ , it should be maintained between  $90^\circ \pm 10^\circ$  and the angle between thigh and calf  $Angle_2$  between  $90^\circ \pm 10^\circ$ . The skeletal segments  $S_{1mid}$  with  $S_{89}$ , the  $S_{1112}$  form  $Angle_1$ ; skeletal segments  $S_{89}$  with  $S_{910}$ , and  $S_{1112}$  with  $S_{1213}$  form  $Angle_2$ . This gives the sitting determination formula definition of the local angle feature as follows.

$$\begin{cases} 0, & 80 \leq Angle_1, Angle_2 \leq 100 \\ 1, & Angle_1, Angle_2 < 80 \text{ or } Angle_1, Angle_2 > 100 \end{cases} \quad (3)$$

Where 0 is correct sitting posture and 1 is poor sitting posture.

Also, consider the constraints made by the global angular characteristics. The  $Angle_3$  formed by the shoulder and ankle to the plane of the ankle when a person is sitting. For a healthy sitting posture,  $Angle_3$  should be maintained between  $14^\circ \pm 10^\circ$ . Skeletal segment  $S_{210}$  with  $S_{10 \text{ 平}}$ , the  $S_{513}$  with  $S_{13 \text{ 平}}$  form  $Angle_3$ . Such a modified the sitting determination formula of global angle feature combined with a local angle feature is as follows.

$$\begin{cases} 0, & 80 \leq Angle_1, Angle_2 \leq 100 \\ & \text{and } 4 \leq Angle_3 \leq 24 \\ 1, & (Angle_1, Angle_2) < 80 \\ & \text{or } (Angle_1, Angle_2) > 100 \\ & \text{or } Angle_3 < 4 \\ & \text{or } Angle_3 > 24 \end{cases} \quad (4)$$

Where 0 is correct sitting posture and 1 is poor sitting posture.

The human sitting information is divided into three feature subsets: skeletal keypoints, global angle features and local angle features. The model is trained by serially using them as multidimensional feature inputs. In this study, a local angle feature is obtained 4 from the angle defined between two skeletal segments, 2 global angle feature, 18 pairs of key points feature, resulting in a 42 dimensional feature vector  $f_i = \{f_1, f_2, \dots, f_{42}\}$ , including 36 human key points features, 4 local angle features, 2 global angle features were obtained in total. The global angle feature is used as a constraint on the local angle feature to capture more detailed information about the sitting angle, and the combination of the global angle feature and the local angle feature provides a more comprehensive representation of the sitting posture.

### C. System Model

The overall system architecture has three components. The data enhancement module, the skeletal feature extraction module and the temporal sitting discrimination module, as shown in Fig 3.

The data expansion process for the data enhancement modules is shown in the Fig 4.

The skeletal feature extraction module consists of OpenPose and a feature extraction mechanism to extract keypoints data, local angle features and global angle features of the human skeleton. The temporal posture discrimination module uses Keras to build an LSTM deep learning model for posture

recognition and classification. The deep learning model has five layers including Lambda, LSTM and 2 Dense layers, and uses Sigmoid as the activation function of output layer. The Dense layer uses tanh as the activation function.

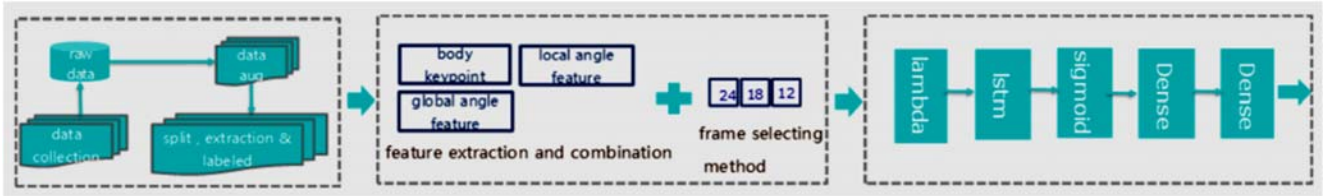


Figure 3. General framework diagram

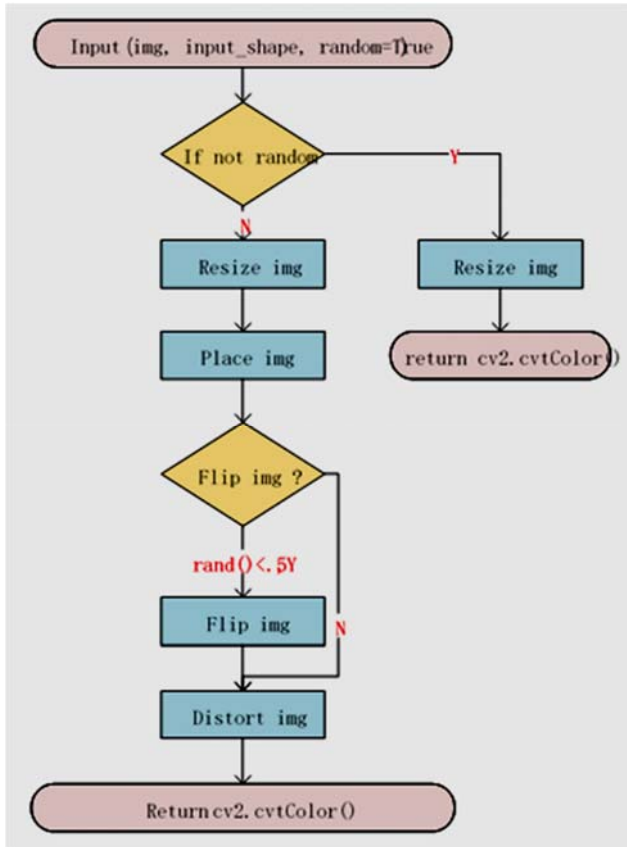


Figure 4. Flow chart of data enhancement method

#### IV. EXPERIMENTAL RESULTS

##### A. Sitting Evaluation Indicators

This paper is a single-category identification of correct sitting posture and poor sitting posture, with recall, precision,

$$recall = \frac{TP}{TP + FN} * 100$$

accuracy, and F1\_score chosen as experimental evaluation indicators.

$$accuracy = \frac{TP + TN}{TP + FP + FN + TN} * 100$$

$$F1\_score = \frac{2 * P * R}{p + R} * 100, \tag{5}$$

where TP is the true class, TN is the true negative class, FP is the false positive class and FN is the false negative class.

For multiple classifications, we use macro-averages and weighted averages as evaluation metrics.

$$Macro\_P = \frac{1}{n} \sum_{i=1}^n P_i,$$

$$Macro\_R = \frac{1}{n} \sum_{i=1}^n R_i, \tag{6}$$

$$Macro\_F = \frac{1}{n} \sum_{i=1}^n F_i,$$

$$Weighted\_P = \sum_{i=1}^n \frac{TP_i + FP_i}{\sum_{i=1}^n TP_i + FP_i} * P_i,$$

$$Weighted\_R = \sum_{i=1}^n \frac{TP_i + FP_i}{\sum_{i=1}^n TP_i + FP_i} * R_i, \tag{7}$$

$$Weighted\_F = \sum_{i=1}^n \frac{TP_i + FP_i}{\sum_{i=1}^n TP_i + FP_i} * F_i,$$

$$precision = \frac{TP}{TP + FP} * 100,$$

Where  $P_i$ ,  $R_i$ ,  $F_i$  denotes the precision, recall,  $F1\_score$ , of the  $i$ th category  $TP_i$  denotes the true class of the  $i$ th category, and  $FP_i$  denotes the false positive class of the  $i$ th category.

*B. Preprocessing of Datasets*

Machine learning and deep learning algorithms are based on massive amounts of data to learn, and models are prone to overfitting problems when the amount of data is insufficient. In this paper, the data enhancement method will use geometric transformations of the original image, such as rotation and scaling, combined with spatial transformations of the original image and replacement fills for the color space to expand the dataset. The dataset is expanded by randomly flipping, reconstructing and scaling the video seated image, and filling the color transformations respectively.

Data augmentation according to the Fig 4 expands the dataset by first determining whether the video frame is random, if it is random then directly re-crop the size of the video frame and then return the color reconstructed video frame. If it is not random, the video frame is first re-cropped in size, then the random number is used to decide whether to flip the video frame, if the random number is greater than the threshold then the image is directly distorted, otherwise the video frame is first flipped before the image is distorted, and finally the color reconstructed video frame is returned. The results of the experiment are shown in Table 2. According to the table it can be seen that before the data enhancement the model fit was almost close to 100% and overfitting occurred, after the data enhancement the model predictions showed normal results.

TABLE II. COMPARISON OF SITTING RECOGNITION BEFORE AND AFTER DATA AUGMENTATION

| row data | before preprocessing data |        |          | after preprocessing data |        |           |
|----------|---------------------------|--------|----------|--------------------------|--------|-----------|
|          | precision                 | recall | F1_score | precision                | recall | precision |
| 0        | 99.72%                    | 99.76% | 99.75%   | 92.00%                   | 95.00% | 93.48%    |
| 1        | 99.75%                    | 99.76% | 99.75%   | 92.00%                   | 94.60% | 93.28%    |

Where 1 is wrong sitting posture, 0 is right sitting posture.

*C. Testing on Different Datasets*

Studies on the laws of human movement have shown that a person can change 2 up to 3 times a second while sitting [30]. The three "gates" of LSTM, "forget gate", "input gate" and "output gate", can selectively retain the important information of the previous t-1, which can solve the problem of gradient disappearance of recurrent neural network. In this study, the video sitting recognition is for continuous time series, and it needs to combine the feature information of the previous t-1 to determine the sitting posture, so LSTM is chosen as the classifier. The loss function uses a binary cross-

entropy loss, which is a good measure of loss and converges quickly and easily, as shown in (8). Optimizer for Adam. The results are shown in the Table III and show that the highest accuracy is achieved when all frames in one second are selected.

$$Cost(A, Y) = \frac{1}{m} \sum_{i=1}^m (-y_i \log(a_i) - (1 - y_i) \log(1 - a_i)) \quad (8)$$

where  $a_i = sigmoid(z_i) = \frac{1}{1 + e^{-z_i}}$ ,  $z_i = w_i^T X_i + b_i$ ,  $m$  is the number of samples,  $y_i$  is the predicted test dataset.

TABLE III. LSTM RESULTS USING DIFFERENT FRAME COUNTS

| Frame/s | Features Extraction Times/s | Accuracy | Recall | F1_score |
|---------|-----------------------------|----------|--------|----------|
| 24      | 259157                      | 98.76%   | 98.86% | 98.88%   |
| 18      | 201454                      | 96.18%   | 96.04% | 96.21%   |
| 12      | 172564                      | 95.07%   | 94.86% | 95.12%   |

Table IV gives the results of the sitting posture recognition accuracy, recall and  $F1\_score$  for different sub-features of the human sitting posture. From the results, it can be seen that the sitting posture recognition accuracy is the highest when the three features are combined together, and the recall and  $F1\_score$  are also the highest.

TABLE IV. RESULTS OF SITTING RECOGNITION USING DIFFERENT FEATURES

| using feature of training | accuracy | recall | F1_score |
|---------------------------|----------|--------|----------|
| only body keypoint        | 94.14%   | 93.63% | 94.18%   |
| only local angle feature  | 92.56%   | 92.08% | 92.59%   |
| only global angle feature | 90.03%   | 89.57% | 90.13%   |
| all features above        | 98.76%   | 98.86% | 98.88%   |

Due to the presence of human key points masked on the public dataset, they could not be identified. For this, the obscured human skeletal key points are processed as follows.

1. defining the proximity key points based on 18 pairs of key points of the human skeletal framework;
2. calculating each masked key point by the relative distance of the adjacent key points according to the human skeletal symmetry and skeletal proportions, with the coordinates of each key point being  $j_i = (x_i, y_i)$ ,  $0 \leq i \leq 17$ ;
3. when  $i$  is in a different range, there are two cases:

$$\text{Situation 1: } \begin{cases} x_i = \frac{x_{[i][1]} - x_{[i][2]}}{2} \\ y_i = \frac{y_{[i][1]} + y_{[i][2]} - 2d}{2} \end{cases}, 0 \leq i \leq 1, \quad (9)$$

Where  $d$  is a constant,  $x_{[i][1]}$ ,  $x_{[i][2]}$  are the x-coordinates of the first and second proximal points of  $j_i$  respectively,  $y_{[i][1]}$ ,  $y_{[i][2]}$  are the y-coordinates of the first and second proximal points of  $j_i$  respectively.

$$\text{Situation2: } \begin{cases} x_i = x_{[i][1]} + t \cdot a \\ y_i = y_{[i][1]} \end{cases}, 2 \leq i \leq 17, \quad (10)$$

Where  $a = 5 \cdot d$ ,  $t_i$  is a list of constants,  $X_{[i][1]}$ ,  $Y_{[i][2]}$  are the coordinates of  $x$ ,  $y$  of the proximal points of  $j_i$  respectively.

The key points of the human skeleton are highlighted in two ways: those on the body's axis of symmetry, such as the nose and chest, and those not on the body's axis of symmetry. For key points on the axis of symmetry we fill in the key points by their proximity to the key points. For key points that are not on the axis of symmetry, they are filled in by the symmetrical key points of the key points.

Table V and Table VI give the results of human pose recognition and classification for the KTH dataset and the Weizmann dataset respectively by processing obscured key points and integrating human skeletal key points, local angle features and global angle features.

TABLE V. TEST RESULTS FOR THE KTH DATASET

|              | precision | recall | F1-Score | accuracy |
|--------------|-----------|--------|----------|----------|
| macro avg    | 94.30%    | 93.00% | 93.65%   | 95.2%    |
| weighted avg | 93.00%    | 94.40% | 93.69%   |          |

TABLE VI. TEST RESULTS FOR THE WEIZMANN DATASET

|              | precision | recall | F1-Score | accuracy |
|--------------|-----------|--------|----------|----------|
| macro avg    | 95.00%    | 96.50% | 95.74%   | 97.1%    |
| weighted avg | 96.20%    | 94.80% | 95.49%   |          |

The Table V and VI show that the metrics for the masked key points in this paper are slightly lower than the unmasked case. For two reasons, one is that the key points on the human symmetry axis are unrecognizable when masked in their entirety; the other is that the symmetry key points are also unrecognizable when masked in their entirety.

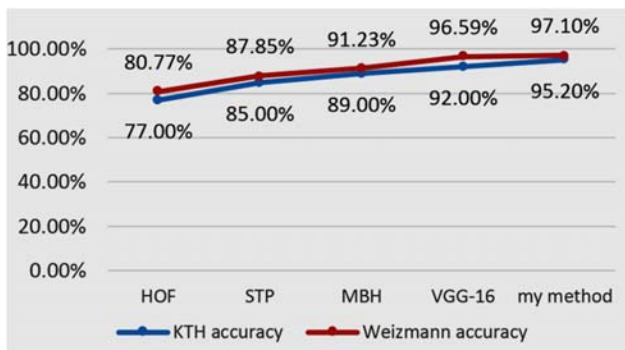


Figure 5. Recognition accuracy of our method and other methods on Weizmann and KTH datasets

Also, key point masking on the symmetry axis and symmetry key points without masking are also not recognized, and thus the test results for the KTH dataset are lower than those tested on the Weizmann dataset. Our method was compared with other methods in the literature using human skeletal key points for human pose recognition and the results are shown in Fig 5.

As can be seen from Fig 5, this paper combines the feature extraction method of human skeletal key points and the LSTM optimization algorithm with high accuracy on a public dataset for human pose recognition, and significantly outperforms other methods using human skeletal data for human pose recognition with good versatility.

## V. CONCLUSIONS

If only a single feature is used it may result in an inadequate amount of information being obtained about the image, which can easily lead to a high uncertainty in the results. However, multiple features can make up for the shortcomings of a single feature and more fully express the information of the sitting features in an image. The integration of multiple features can allow single features to complement each other and improve the performance of image classification and recognition. Human skeleton key points features and local angle features can be used to judge the overall sitting posture correctly or incorrectly, and global angle features as a supplement to local angle features can capture more detailed sitting angle information for sitting posture judgement. Experiments show that the use of human skeletal multidimensional features for sitting posture recognition compensates for the lack of information in a single feature and effectively improves the accuracy of sitting posture recognition. Also, compared with other methods using human skeletal information for human posture recognition, the method in this paper has a high recognition accuracy on human posture dataset and has good generality.

Due to the variable nature of human sitting movements, the sitting criteria selected in this paper are not able to identify the weak angular changes in local angles well. In further research, we will try to use spatial information, three-dimensional coordinates for sitting posture recognition and judgement.

## REFERENCES

- [1] Punnett L , Wegman D H . "Work-related musculoskeletal disorders: the epidemiologic evidence and the debate." *Journal of Electromyography & Kinesiology Official Journal of the International Society of Electrophysiological Kinesiology*, vol.14, pp.13-23,2004.
- [2] Hoogendoorn W E , Bongers P M , Vet H D , et al. "Flexion and Rotation of the Trunk and Lifting at Work are Risk Factors for Low Back Pain: Results of a Prospective Cohort Study." *Spine*, vol.25, pp. 3087-3092, 2014.
- [3] Zheng Yanxia, Zheng Dachuan. A method and device for detecting and correcting sitting posture.; CN. Patent 110717392A, 2020.
- [4] Zhang Y, Zheng TH, Zhang ZH, et al. "Sitting posture detection device and sitting posture detection method." CN. Patent 112633411A,2021.

- [5] Zhao Xiong, Chen Ping, Pan Jinxiao. "A method for identifying abnormal behavior in vehicles based on skeleton key points." *Mechanics and Electronics*, vol.39, pp.6-8, 2021.
- [6] Chandna, S.; Wang, W. "Bootstrap Averaging for Model-Based Source Separation in Reverberant Conditions." *IEEE Trans. Audio Speech Lang. Process*, Vol.26, pp.806-819, 2018.
- [7] Lis, A.M.; Black, K.; Korn, H.; Nordin, M. "Association between Sitting and Occupational LBP." *Eur. Spine J*, vol.16, pp. 283-298, 2007.
- [8] Zhang Z., Yang B. "Application of Head Pose Estimation based on Combination with Particle Filter Algorithm and Mean Shift." *International Journal of Simulation: Systems, Science & Technology*, vol.19, pp. 1-5, 2015.
- [9] Tak W, Pala L. "An Unsupervised Approach for Human Activity Detection and Recognition." *International Journal of Simulation: Systems, Science & Technology*, vol.5, pp.42-49, 2014.
- [10] O'Sullivan, P. B.; Grahamslaw, K.M.; Lapenskie, S.C. "The Effect of Different Standing and Sitting Posture on Trunk Muscle Activity in a Pain-free Population." *Spine*, vol.27, pp. 1238-1244, 2002.
- [11] Abd A, El E et al. "Sign Language Hand Gesture Recognition Using Autoencoder and Support Vector Machine Classifiers." *International Journal of Simulation: Systems, Science & Technology*, vol.5, pp.1-9, 2020.
- [12] Straker, L.; Mekhora, K. "An Evaluation of Visual Display Unit Placement by Electronmyography, Posture, Discomfort and Preference." *Int. J. Ind. Ergon*, vol.26, pp. 389-398, 2000.
- [13] Grandjean, E.; Hünting, W. "Ergonomics of Posture-review of Various Problems of Standing and Sitting Posture." *Applied Ergonomics*, vol.8, pp.135-140, 1977.
- [14] H. Z. Tan, L. Slivovsky, and A. Pentland. "A sensing chair using pressure distribution sensors, Mecha-tronics." *IEEE/ASME Transactions on*, vol.6, pp. 261-268, 2001.
- [15] M. Zhu, A. M. Martinez, and H. Z. Tan. "Template-based recognition of static sitting postures, in Com-puter Vision and Pattern Recognition Workshop." *Conference on Computer Vision & Pattern Recognition Workshop. IEEE*, 2003, pp.50-50.
- [16] Ribeiro, B, et al. "Optimization of sitting posture classification based on user identification." *Bioengineering IEEE*, 2015, pp.1-6.
- [17] B. Mutlu, A. Krause, J. Forlizzi, C. "Guestrin, and J. Hodgins, Robust, low-cost, non-intrusive sensing and recognition of seated postures." *Acm Symposium on User Interface Software & Technology. ACM*, 2007, pp.149-158.
- [18] J. Meyer, B. Arnrich, J. Schumm, and G. Troster. "Design and modeling of a textile pressure sensor for sitting posture classification." *IEEE Sensors Journal*, vol.10, pp.1391-1398, 2010.
- [19] W. Xu, Z. Li, M.-C. Huang, N. Amini, and M. Sarrafzadeh. "ecushion: An etextile device for sitting posture monitoring". *International Conference on Body Sensor Networks. IEEE*, 2011, pp. 194-199.
- [20] Jaimes, Alejandro. "Sit straight (and tell me what I did today): a human posture alarm and activity summarization system." *Acm Workshop on Continuous Archival & Retrieval of Personal Experiences ACM*, 2005, pp.23-34.
- [21] Cheng Yaoyu, Feng Jing, Li Shujun, et al. "A face detection based on Haar and skin color segmentation algorithm." *Journal of Arms and Equipment Engineering*, vol.5, pp.42-45, 2021.
- [22] Jia Ruochen. "Research on human sitting posture feature extraction and recognition algorithm based on machine vision technology." M.A. thesis, Harbin University of Technology, China, 2015.
- [23] Cai Shiqi. "Research on human skeleton extraction and sitting posture recognition based on Kinect." M.A. thesis, Wuhan University of Technology, China, 2018.
- [24] Li S S. "Design and Implementation of Sitting Position Recognition Software Based on Kinect Sensor." M.A. thesis, University of Electronic Science and Technology, China, 2018.
- [25] Le T L, Nguyen M Q, Nguyen T M. "Human posture recognition using human skeleton provided by Kinect". *International Conference on Computing. IEEE*, 2013, pp.340-345.
- [26] Chen K. "Sitting Posture Recognition Based on OpenPose." *IOP Conference Series Materials Science and Engineering*, 2019, 677-682.
- [27] Tu J. "Do you know the correct sitting posture." *Health and Life*, vol.1, pp. 17-20, 2018.
- [28] O "Sullivan K, O "Sullivan P, O "Sullivan L, et al. "What do physiotherapists consider to be the best sitting spinal posture?" *Manual Therapy*, vol.17, pp.432-437, 2012.
- [29] Donald, D, Harrison, et al. "Sitting biomechanics Part I: Review of the Literature." *Journal of Manipulative and Physiological Therapeutics*, vol.22, pp. 594-609, 1999.
- [30] Zhang Hui, Xue Qiang, Wang Xingtao. "Study on the trajectory of human sit-to-stand transition movement based on knee support." *Chinese Rehabilitation Theory and Practice*, vol.6, pp.7-10, 2020.